RANDOM MAGNETIC FIELD EFFECTS ON ELECTRONIC PROPERTIES IN SUBSTITUTIONALLY AND TOPOLOGICALLY DISORDERED ALLOYS.

A. HOUARI, N. BENACHOUR and A.F.R. DIB

Faculté des Sciences.
Département de Physique.
Université de Tlemcen, 13000. ALGERIA

We numerically investigate the effects of the random static magnetic field on a variety of electronic properties (*localization of electron wavefunctions, spectral correlations and electrical conductance*) in substitutionally and topologically disordered alloys. For this, we generate two-dimensional substitutionally disordered alloys and simulate three-dimensional amorphous structures by a molecular dynamics algorithm. As Hamiltonian models, we use the usual Anderson tight-binding model for the substitutional disorder and a tight-binding model with a set of explicit s-type orbitals for the topological disorder.

We particularly focus on the effect of the random magnetic field on the localization of electron wavefunctions. In the presence of the substitutional disorder, we establish that the random magnetic field tends to delocalize the electron wavefunctions at the band center less than does the uniform magnetic field and it enhances the localization at the band edges. But, in the presence of the topological disorder, we observe the opposite effect. We show that the random magnetic field tends to delocalize the electron wavefunctions more than does the uniform magnetic field. In this respect, we demonstrate that the effect of the random magnetic field on the electron wavefunctions depends on the nature of the disorder.

PACS : 71.15.Pd, 71.55.Jv, 72.10.-d, 72.15.-v, 72.15.Rn

I.Introduction:

The localization problem in the random magnetic field has attracted a strong interest for some
time now. The main motivation behind this interest is the established connection between the gauge field theory applied to the highly correlated electron systems in two-dimensions (2D) and the problem of the electron wavefunctions in the presence of the random gauge flux or equivalently the random magnetic field. Particularly, it has been demonstrated that the 2D motion of a single particle in a random magnetic field is related to the slave-boson description of high T_c superconductors [1] and the Chern-Simons theory of the half-filled Landau level [2]. Moreover, experimentalists are now dealing with measurements of transport properties in a static random magnetic field and this reinforces the present interest to this subject [3].

e-mail : a_houari@yahoo.fr

According to the scaling theory of localization [4], all the wavefunctions of a 2D system are exponentially localized in the absence of a magnetic field, however weak the disorder is. Since the presence of a magnetic field destroys the time-reversal symmetry, this will stand against localization. Nevertheless, pertubative renormalization group calculations show that all states remain localized [5].

To investigate the effect of the random magnetic field on the localization of electron wavefunctions, many authors have tackled this problem. Using Mackinnon's finite size scaling method, T. Sugiyama and N. Nagaosa [6] found that all the wavefunctions in 2D are localized in a random magnetic field. More recently, J. Verges [7], based on a statistical analysis of conductance data, he evaluated directly the localization length for Hamiltonians describing random magnetic fluxes. He basically obtained a substantial increase of the localization length. Also, in one of our numerical works, originally performed for

investigating conductance fluctuations in 2D mesoscopic disordered systems [8,9], we systematically examined localization effects in 2D finite samples. We found that electron wavefunctions *look extend* near the band center and they are *exponentially localized* at the band edges. This strongly suggests the occurrence of mobility edges but we did not focus on their precise locations across the energy band and we did not characterize the nature of the wavefunctions at these mobility edges.

While theory points towards localization, numerical work has not led to a consensus of opinion. Bearing this in mind, we intend in the present work to shed some light on this problem in order to clarify the situation. Therefore and along the lines of the work of J. Verges [7], we numerically investigate the effects of the random magnetic field on a variety of electronic properties (localization of wavefunctions, spectral correlations and electrical conductance) in disordered samples. For this, we use two models for the atomic structure and two tight-binding Hamiltonian models for the electronic structure. To the best of our knowledge, we numerically investigate for the first time the random magnetic field effects in realistic topologically disordered systems simulated by a molecular dynamics algorithm. The magnetic field is randomized according to the binary and uniform distributions of its values.

We examine the localization of the wavefunctions by computing the participation ratio [10] of the electron states, a quantity, which essentially measures the spatial extent of the electron states. In addition, to characterize the electric conduction regime in our samples, we use in conjunction with the participation ratio other criteria such as the nearest-neighbor level spacing distribution, the electrical conduction and its distribution.

II. Models of the Disorder and of the Electronic Structure:

Our simplest structure is a regular lattice. In this situation, the disorder is a consequence of the random distribution of two species of potentials on the lattice sites. Topological disorder is modeled by simulating amorphous binary alloys using a molecular

dynamics algorithm based on the Lennard-Jones potential. For this, we consider binary alloys made of N_1 atoms of mass m_1

$$v_{\alpha\beta} = 4\varepsilon\left[\left(\frac{\sigma_{\alpha\beta}}{r}\right)^{12} - \left(\frac{\sigma_{\alpha\beta}}{r}\right)^{6}\right]$$

and diameter $\sigma_1 = \sigma$ and N_2 atoms of mass m_2 and diameter σ_2. Two atoms separated by a distance r are supposed to interact through the Lennard-Jones potential given by :

where α and β are the species indexes and equal to 1 or 2. ε and $\sigma_{\alpha\beta}$ are parameters

with dimensions of energy and length,

$$\sigma_{\alpha\beta} = \frac{1}{2}\left(\sigma_\alpha + \sigma_\beta\right)$$

respectively. The parameter $\sigma_{\alpha\beta}$ is assumed to be :

To avoid the discontinuity of interatomic forces at the cut-off radius of the potential, we modify the Lennard-Jones potential by a cubic spline [11]. Our molecular dynamics simulation is performed in the canonical ensemble following Nosé-Hoover approach which uses the extended system scheme [12]. We numerically integrate the equations of motion by using Trotter factorization [13] of Liouville operator to obtain a stable and time-reversible algorithm. In our simulations, we choose N_2/N_1 =1, m_2/m_1 =2 and σ_2/σ_1 =1.2. The reason for this choice is that it is known that the system with these parameters bypasses crystallization, that is, the system stays in a glassy state for a long time at low temperature [14]. The total number of particles that we used is N =500. The reduced density of the alloys $\rho^* = N\sigma^3/V$ was taken to be 0.85 which is appropriate to glassy behavior. The microscopic time scale is chosen to be $\tau = (m_1\sigma^2/\varepsilon)^{1/2}$. If species 1 is

assumed to be argon, we have $\tau = 3.112X10^{-13}$ s by substituting the parameters appropriate to argon (ε/k_B = 119.8 K, k_B being the Boltzmann constant, $m_1 = 6.63\ X10^{-26}$ Kg and $\sigma = 3.405\ \mathring{A}$) into the expression of τ. The temperature is scaled by ε/k_B. Our structures are simulated in a cubic cell with periodic boundary conditions. The initial configuration is chosen to be the faced centered cubic structure where atoms of both species are placed randomly on the lattice sites of this structure. The reduced temperature is taken to be equal to 0.1 and the time step in the simulations is set $\Delta t/\tau = 0.001$.

As models for the electronic structure, we first use the traditional Anderson tight-binding Hamiltonian model [15] given in 2D by

$$H = \sum_{lm} \varepsilon_{lm} |lm\rangle\langle lm| + \sum_{lm,l'm'} V_{lm,l'm'} |lm\rangle\langle l'm'|$$

where l,m denote the sites of a 2D square lattice and correspond to x and y coordinates respectively. $|lm\rangle$ denotes the eigenstate associated with the site (l,m). The site energies ε_{lm} vary randomly from site to site according to the binary alloy probability distribution:

$$P(\varepsilon_{lm}) = x\delta(\varepsilon_{lm} - \varepsilon_A) + (1-x)\delta(\varepsilon_{lm} - \varepsilon_B)$$

where ε_A and ε_B being the site energies characterizing the chemical species of the alloy. Here, we consider only the diagonal disorder so the hopping matrix elements $V_{lm,l'm}$ are independent of the chemical occupation of the sites (l,m) and (l',m') i.e. $V_{lm,l'm'} = V$ where V is a constant. A uniform magnetic field *B* perpendicular to the system is included in the form of the Peierls phase factor in the hopping matrix elements as follows:

$$V_{lm,l'm'} = \begin{cases} V & \text{if } m = m' \text{ and } l = l' \pm 1 \\ V \exp\left(\pm 2\pi i l \dfrac{\phi}{\phi_0} \right) & \text{if } l = l' \text{ and } m = m' \pm 1 \\ 0 & \text{otherwise} \end{cases}$$

where $\phi = Ba^2$ is the magnetic flux entering a unit cell of the square lattice, a is the lattice constant and $\phi_0 = h/e$ is the flux quantum.

Secondly, we use a Hamiltonian which is defined in real space in terms of potentials

$$H = \frac{p^2}{2m} + \sum U_i = \frac{p^2}{2m} + \sum_i U(r - R_i)$$

U_i centered at each site R_i of a chosen atomic structure i.e.

These potentials U_i represent local impurity potentials felt by electrons in our amorphous samples. This Hamiltonian model has already been used with success in studying conductance fluctuations in two-dimensional and quasi-one dimensional conductors with substitutional disorder [8,9] and in investigating the Hall effect in topologically disordered materials [16].

The analytic form of each potential relative to its center is given by [17]

$$\boldsymbol{U}(\boldsymbol{r}) = -\frac{\boldsymbol{be}^{-\boldsymbol{qr}}}{1 - \boldsymbol{e}^{-\boldsymbol{qr}}}$$

in the limit $b \to \infty$, $q \to \infty$ with $b/q^2 \to ½$ and with units such that $\hbar$=m=e=1. This is convenient because it determines U by only one parameter γ given by $b = \gamma q + \gamma^2/2$. The potential U then has only one bound state at energy $E = -\gamma^2/2$ with wavefunction $\phi(r) = (\gamma/2\pi)^{1/2} exp(-\gamma r)/r$.

We then use the set $\{\phi_i(\mathbf{r}-\mathbf{R}_i)\}$ as basis functions for a tight-binding expansion. This yields matrix elements for the Hamiltonian H_0 (in the absence of a magnetic field *B*) and for the overlap matrix S which have simple forms given in detail in [8]. In the presence of a weak magnetic field *B* in the z-direction, the Hamiltonian is augmented by an additional purely imaginary term H_B with matrix elements linear in *B* whose form is given in [9]. Mathematically, our Hamiltonian matrices are either symmetric or hermitian random matrices depending on

$$\psi_m(\vec{r}) = \sum_i a_{mi}\phi_i(\vec{r} - \vec{R}_i)$$

the absence or the presence of the magnetic

field. The matrix diagonalization procedure is performed by using standard routines given in detail in [18] to obtain all the eigenfunctions and their corresponding eigenvalues. This step in our investigation is a very intensive numerical task particularly with increasing system size [19]. The numerical procedure gives eigenfunctions of the form :

As defined in [10], the participation ratio of the tight-binding wavefunctions ψ_m is given

$$PR_m = \frac{\left[\sum_i |a_{mi}|^2\right]^2}{N\sum_i |a_{mi}|^4}$$

in terms of the N coefficients a_{mi} as
a quantity which is used as a measure of the degree of localization of the wavefunctions.

III. The Kubo Formula for Conductivity:

Using the tight-binding wavefunctions, it is straightforward to evaluate numerically the conductance, using Kubo formula for the diagonal element of the conductivity tensor σ_{xx} .
To evaluate σ_{xx} , we start from its corresponding Kubo expression for finite systems whose energy spectra are discrete. In the actual computation, we must compensate for the discreteness of energy spectra by giving each delta function in the Kubo formula a finite width ε. Therefore, σ_{xx} is given in [8] by

$$\sigma_{xx}(E) = \frac{he^2}{\Omega}\frac{1}{\varepsilon^2}\sum_{l,m}{}' \left|\langle \psi_l | v_x | \psi_m \rangle\right|^2$$

where Ω is the volume of the system, v_x is the velocity operator, x is the position operator and $|\psi_m\rangle$ are the eigenfunctions of the Hamiltonian in the absence of the magnetic field. The primed sums extend over only states within a window of width ε around the energy E.

IV. Computational Aspects:

Our numerical investigation is undertaken with a set of the following parameters: the lattice constant a for the case of the substitutional disorder, the atomic density ρ^* for the case of the topological disorder, the alloy concentration x_A (x_B=1-x_A), the site energies ε_A, ε_B and the magnetic field strength B. We recall here that, with the Anderson tight-binding Hamiltonian model, the magnetic field B is introduced through the flux $\phi = Ba^2$ entering the unit cell in the lattice and it is explicitly introduced in the case of our version of the tight-binding model with the set of explicit atomic orbitals [9].
The choice of parameters was made to enable us to compute the d-c conductivity σ_{xx} in the weak and strong scattering regimes. The scattering regime in our systems is controlled by the scattering strength $\delta \propto |\varepsilon_A - \varepsilon_B|$ and the alloy concentration x_A. We set the constant V = 1 and the lattice constant a =1 for the substitutionally disordered alloys. Our topologically disordered systems are amorphous binary alloys simulated with an atomic density ρ^*=0.85 appropriate to glassy behavior. In our computations, we vary the scattering strength δ, the alloy concentration x_A, the system-size and the energy. We average all computed quantities over the disorder. To characterize the scattering regime in our systems, we evaluate the participation ratio of the wavefunctions and the dimensionless conductance g across the energy spectrum. The weak scattering regime in a given system is achieved for PR ~ 1/3 [20] and a value of g >> 1. However, the strong scattering regime takes place whenever PR is ∂ ($1/N$) (N being the number of sites in the system) and g ~ 1 corresponding to the threshold for the metallic behavior.

Results and Discussion:

As a preliminary step, we tested the standard routines [18] which we used in solving the eigenvalue problem corresponding to the Schrödinger equation. For this, we solved this eigenvalue problem using the Anderson tight-binding model on a 2D periodic square lattice with the following parameters: the site energy $\varepsilon = -2$, the system-size = LXL =20X20. Basically, we obtained a set of stationary waves and highly degenerate eigenstates by computing the nearest-neighbor level spacing distribution. These results are characteristic of the periodic systems.

To examine the effect of the random magnetic field on the localization of wavefunctions, we computed the participation ratio (*PR*) of all the eigenstates in a 2D substitutionally disordered binary alloys having the following parameters: $\varepsilon_A = 0.5$; $\varepsilon_B = -0.5$, $x_A = x_B = 0.5$ and a sample-size = LXL = 30X30. Fig.(1) shows the disorder-averaged *PR* versus the energy in the absence and the presence of uniform and the random magnetic field. We simply randomize the magnetic field *B* by taking the values of the flux ϕ randomly according to the binary distribution i.e. $\phi = \phi_0$ or $-\phi_0$. The data shown by Fig.(1) are averages over 30 independent disorder realizations. First, we identified the nature of the wavefunctions across the energy band on the basis of the size-dependence of the *PR*. With the chosen parameters, we found states are extended near the band center (PR ~ 0.3

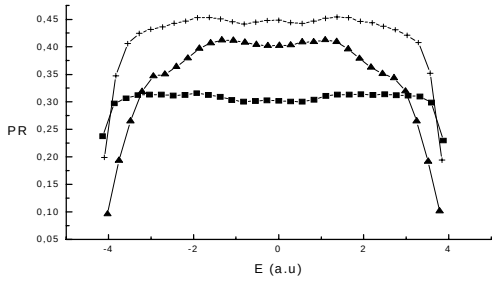

Figure(1): The averaged participation ratio versus energy for a 30X30 substitutionally disordered binary alloy in the absence and the presence of the uniform and the random magnetic field. (+) Uniform magnetic field; (▲) Random magnetic field, (■) Zero magnetic field.

around E ~ 0) and exponentially localized at the band edges ($PR \sim \partial (1/N)$ at $|E| \sim 4$). In the presence of the uniform magnetic field *B*, we observe a substantial increase of *PR* ($PR_B \sim 0.45$) near the band center and a small decrease of *PR* near the band edges. This means that the magnetic field delocalizes the wavefunctions near the band center and it enhances their localization at the band edges. The delocalization effect of the wavefunctions near the band center is due to the destruction of the phase coherence of the wavefunctions by the application of the magnetic field. The localization enhancement of the wavefunctions near the band edges can be understood by invoking the following analogy. Since wavefunctions are exponentially localized near the band edges, a magnetic field will enhance their localization in the way that a magnetic field will shrink the atomic orbital of the electron in the hydrogen atom [21]. In the presence of the random magnetic field, we observe a net decrease in the value of *PR* compared to its value in the presence of the uniform magnetic field along the entire bandwidth. Therefore, the random magnetic field has the tendency to delocalize the wavefunctions less than does a uniform magnetic field. We can understand this fact as follows: intuitively, the random aspect in the distribution of the values of the magnetic field makes the occurrence of the destruction of the phase coherence of the wavefunctions also random. Consequently, this will affect the localization of the wavefunctions, which will be less pronounced than in the case of the uniform magnetic field.

We also used the uniform distribution of the random magnetic field for comparison. We point out here that the uniform distribution of the magnetic flux is the most frequently used distribution in previous numerical works of the present subject. We randomly varied the flux ϕ uniformly in the interval $[-\phi_0, \phi_0]$. Fig.(2) shows the disordered-averaged *PR* versus energy using both distributions of the random magnetic field and with the same parameters used for

obtaining Fig.(1). Fig.(2) clearly indicates that a random magnetic field with a uniform

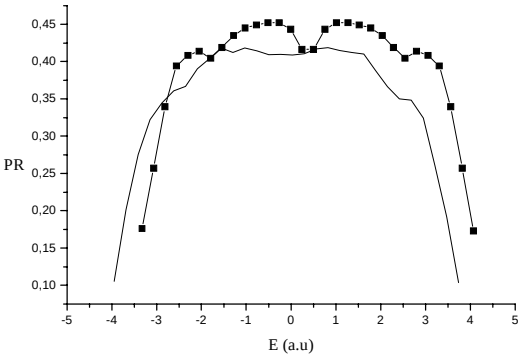

Figure(2): The averaged participation ratio versus energy for a 30X30 substitutionally disordered binary alloy in the random magnetic field. (■) Random magnetic field with the binary distribution, (—) Random magnetic field with the uniform distribution.

distribution has the tendency to delocalize the wavefunctions less than does a random can understand this effect by the fact that the uniform distribution introduces more randomness in the values of the magnetic field than does the binary distribution. Consequently, the phase coherence of the wavefunctions will be less destructed in a random magnetic field with a uniform distribution than in a random magnetic field with a binary distribution.

Fig.(3) shows the histograms of the nearest-neighbor level spacing distribution for substitutionally disordered alloys in the absence of the magnetic field (Fig.3-a) and the presence of the random magnetic field (Fig.3-b) with a uniform distribution. Fig.(3-a) and Fig.(3-b) are obtained with the set of the following parameters : $\varepsilon_A = 0.5$; $\varepsilon_B=-0.5$, $x_A=x_B=0.5$ and a sample-size =LXL=35X35.

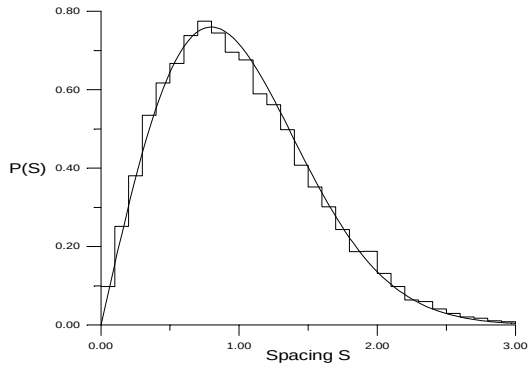

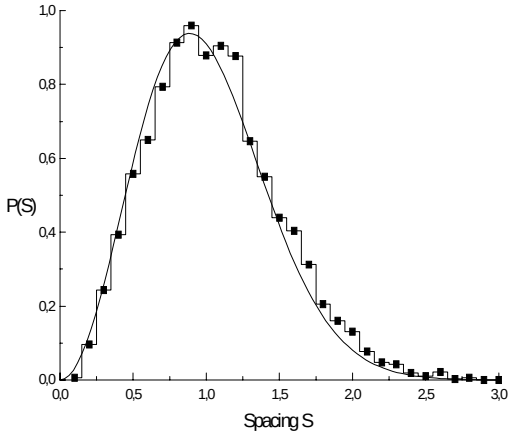

(a)

(b)

Figure(3): The histograms of the nearest-neighbor level spacing distribution for a 35X35 substitutionally disordered binary alloy. (a): in the absence of the magnetic field. (b): in the presence of the random magnetic field with a uniform distribution.The fitting curves are the Wigner-Dyson distributions for the G.O.E. universality class (a) and the G.U.O. universality class(b).

Fig.(3-b) we clearly shows that a random magnetic field induces a transition in the nearest-neighbor level spacing distribution in a weakly disordered system from the Gaussian Orthogonal Ensemble (*G.O.E.*) universality class to the Gaussian Unitary Ensemble (*G.U.E.*) one. Fig.(4) shows the electrical conductance versus energy in the

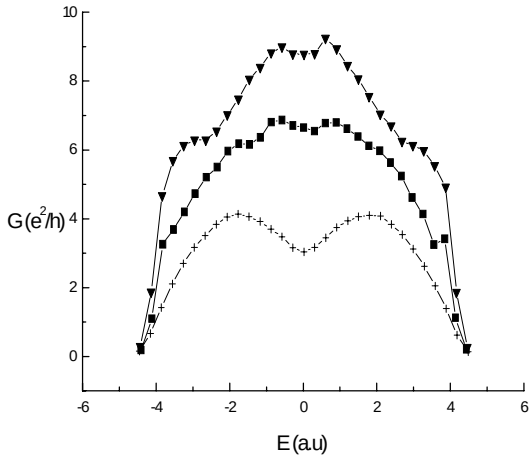

Figure(4): The averaged electrical conductance versus energy for a 35X35 substitutionally disordered binary alloy in the absence and the presence of the uniform and the random magnetic field. (▾) Uniform magnetic field; (■) Random magnetic field, (+) Zero magnetic field.

absence and the presence of the magnetic field for the substitutionally disordered alloys with the set of the following parameters: ε_A = -1.; ε_B=+1., x_A=x_B=0.5 and a sample-size =LXL=35X35. Fig.(4) confirms the trend shown by the variation of *PR* in Fig.(1). The electrical conductance g increases in the presence of the random magnetic field compared to its value in the absence of the magnetic field but it decreases as a consequence of the net decrease in the value of *PR* with respect to its value in the presence of the uniform magnetic field.

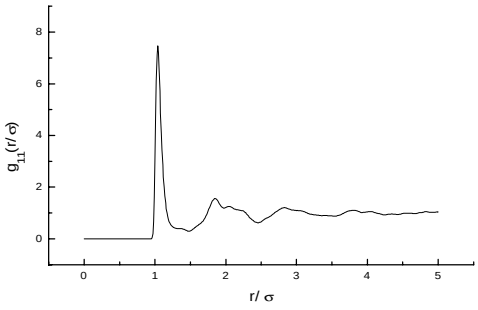

(a)

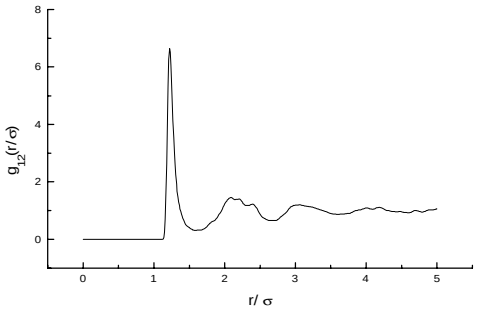

(b)

Figure(5): The radial distribution function g(r) for our simulated amorphous binary alloys. The interatomic distances r are in units of the diameter σ of the species 1. For details of the structures, see the text. (a) : the radial distribution function $g_{11}(r)$ between the same species 1. (b) : the radial distribution function $g_{12}(r)$ between species 1 and species 2 concentration x_A (x_B=1-x_A) and the magnetic field strength *B*.

To test the effect of the nature of the disorder, we used topologically disordered systems which we described above to investigate the localization of electron wavefunctions in the presence of the random magnetic field. Fig.(5) shows typical radial distribution functions g(r) of our simulated topologically disordered systems. With the topological disorder, the relevant parameters are the site potentials γ_A; γ_B , the alloy

Representative results of the computation of the disorder-averaged *PR* as a function of energy in the absence and the presence of the magnetic field are shown in Fig.(6). The data shown in Fig.(6) are obtained with the following parameters : γ_A=2. ; γ_B = 1.75, x_A= 0.5, a sample-size N= 500 and are averages over 10 independent disorder configurations. The magnetic field is taken to be constant B=0.02 in atomic units (*a.u.*) for the uniform case and randomly distributed according to the binary distribution for the random case. Fig.(6) shows that, in topologically disordered systems, a random magnetic field has the tendency to delocalize the wavefunctions more than does a uniform magnetic field. We must stress here that this result is contrary to what we obtained in 2D susbtitutionally disordered alloys. Here again, we checked the condition of the electric conduction in our topologically disordered samples. We computed the electric conductance across the entire bandwidth and obtained a value of g ~ 10 near the band center which is an indication of the metallic regime. We also computed the nearest-neighbor level spacing distribution in the absence and the presence of the magnetic field and we found that it follows the Wigner-Dyson distribution, which is again a signature of the weak disorder situation.

In this work, based on the inspection of the spatial behavior of the electron

wavefunctions, we first showed that a random magnetic field delocalizes the extended states less than does a uniform magnetic field and it enhances the degree of localization of localized states in 2D substitutionally disordered alloys. In this

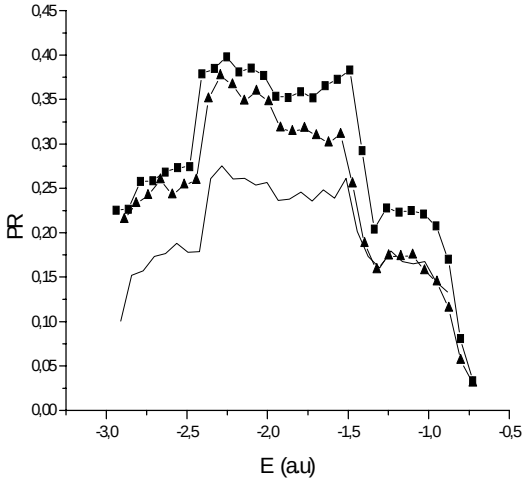

Figure(6): The averaged participation ratio versus energy in an amorphous binary alloy with 500 atoms in the absence and the presence of the uniform and the random magnetic field. (▲) Uniform magnetic field; (■) Random magnetic field, (—) Zero magnetic field.

respect, although we did not evaluate the localization length out of our present models, we confirmed the finding of J. Verges [7] who directly extracted the localization length and observed an increase in its value in the presence of the random magnetic field. Secondly, we showed that a random magnetic field, however weak it is, induces a transition in the nearest-neighbor level spacing distribution from the *G.O.E.* universality class to the *G.U.E.* one in 2D substitutionally disordered alloys. Most important, we clearly demonstrated that the effect of the random magnetic field on the electron wavefunctions depends on the type of disorder. Presumably, this fact has to do with the nature of the wavefunctions themselves in each type of the disorder. In order to clarify here the role of the topological disorder, we must understand the interplay of the effects of random magnetic field and the topological disorder. Also, we should examine the effects of the different distributions of the magnetic field in more detail in both types of the disorder. We intend to carry out such a study in the near future.

References

[1] Ioffe, L.B. and Larkin, A.I., Phys. Rev. B **39**, 8988 (1989); Lee, P.A., Phys. Rev. Lett. **63**, 680 (1989); Nagaosa, N. and. Lee, P.A, *ibid*. **64**, 2450 (1990).

[2] Kalmeyer, V. and Zhang, S.C., Phys. Rev. B **46**, 9889 (1992); Halperin, B.I., Lee, PA. and Read, N., *ibid*. **47**, 7312 (1993).

[3] Mancoff, F.B., Zielinski, L.J., Marcus, C.M., Campman, K. and Gossard, A.C. Phys. Rev. B **53**, R7599 (1996).

[4] Abrahams, E., Anderson, P.W., Licciardello, D.C. and Ramakrishnan, T.V., Phys. Rev. Lett. **42**, (1979) 673.

[5] Aronov, A.G., Mirlin, A.D. and Wölfle, P., Phys. Rev. B **49**, 16609 (1994).

[6] Sugiyama, T. and Nagaosa, N., Phys. Rev. Lett. **70**, 1980 (1993).

[7] Verges, J.A., Phys. Rev. B **57**, 870 (1998).

[8] Harris, R. and Houari, A., Phys. Rev. B **41**, 5487 (1990).

[9] Harris, R. and Houari, A., Phil. Mag. B **65**, 1131 (1992).

[10] Edwards, J.T. and Thouless, D.J., J. Phys. C **5**, 807 (1972).

[11] Erpenbeck, J.J., Phys. Rev. A **38**, 6255 (1988).

[12] Nosé, S., Pro. Theor. Phys. Supp. **103**, 1 (1991).

[13] Tuckerman, M.E., Tobias, D.J. and Klein, M.L., Mol. Phys. **87**, 5 (1996).

[14] Fujiwara, S. and Yonezawa, F., Phys. Rev. Lett. **54**, 644 (1995).

[15] Anderson, P.W., Phys. Rev. **109**, 1492 (1958).

[16] Houari, A., Mebrouki, M., Dib, A.F.R. and Ould-Kaddour, F., Physica B : Cond. Matt. **291** 387 (2000).

[17] Berezin, A.A., Phys. Rev. B **33**, 2122 (1985).

[18] Press, W.H., Flannery, B.P., Teukolsky, S.A. and Vetterling, W.T., ‘‘Numerical Recipes’’ (Cambridge University Press 1986).

[19] The standard algorithms used to solve for our real and complex generalized eigenvalue problem H X= λSX are very stable and accurate. About 1 hour CPU time is needed for matrices with a size 900 X 900 on a microcomputer with PIV processor. A large RAM memory is also necessary.

[20] As discussed in Ref. [10], the value 1/3 corresponds to the coefficients a_{mi} of the tight-binding wavefunctions being distributed in an approximately gaussian manner for each wavefunction.

[21] Ando, T., Phys. Rev. B **42**, 5325 (1989).